



# Vertebral bone marrow edema in magnetic resonance imaging correlates with bone healing histomorphometry in (sub)acute osteoporotic vertebral compression fracture

Yun Zhang<sup>1</sup> · Haoran Qi<sup>2</sup> · Yefeng Zhang<sup>2</sup> · Junning Wang<sup>1</sup> · Jingcai Xue<sup>3</sup>

Received: 17 August 2020 / Revised: 20 January 2021 / Accepted: 7 March 2021 / Published online: 20 March 2021  
© The Author(s), under exclusive licence to Springer-Verlag GmbH Germany, part of Springer Nature 2021

## Abstract

**Background** BME on MRI has become the gold standard for the diagnosis of acute/subacute OVCF, but the correlation between the quantitative model of BME and histopathological manifestations of OVCF is rarely discussed in the literature.

**Objectives** This study aimed to retrospectively investigate the relationship between bone marrow edema (BME) in magnetic resonance imaging (MRI) and bone healing histomorphometry in (sub)acute osteoporotic vertebral compression fracture.

**Methods** According to the period since fracture, 125 patients were divided into four stages: stage I (0 to 15 days), stage II (16 to 30 days), stage III (31 to 60 days) and stage IV (61 to 90 days). Bone marrow edema was evaluated by the signal changes and intensity patterns on MRI sagittal images. Decalcified biopsy specimens were obtained from the cancellous bone core in the fractured vertebral body. The histomorphometry study results were analyzed by light microscopy using grid analysis and defined using bone histomorphometry criteria.

**Results** There were 70 (56%) patients in stage I, 29 (23.2%) in stage II, 12 (9.6%) in stage III and 14 (11.2%) in stage IV. BME and histomorphometry characteristics differentiated from each other stage: The BME percentage had a significantly negative correlation with the ratio of osteoid volume/bone volume ( $r = -0.539$ ,  $p = 0.001$ ) and the ratio of woven bone volume/tissue volume ( $r = -0.584$ ,  $p = 0.001$ ). There was also a positive correlation between the BME percentage and the ratio of fibrous tissue volume/tissue volume ( $r = 0.488$ ,  $p = 0.001$ ).

**Conclusions** Bone marrow edema significantly correlates with bone morphology parameters after vertebral fracture. The characteristics of histomorphological changes during fracture healing process can be preliminarily determined by observing the edema signal.

**Keywords** Osteoporotic vertebral compression fracture · Bone marrow edema · Bone histomorphometry

---

Because Yun Zhang and Haoran Qi contributed equally to this article, Yun Zhang and Haoran Qi are simultaneously co-first authors.

✉ Jingcai Xue  
spine2000@msn.cn

<sup>1</sup> Department of Geriatrics, Shandong University of Traditional Chinese Medicine, Jinan 250021, People's Republic of China

<sup>2</sup> Department of Spine, Shandong Provincial Hospital Affiliated To Shandong University, Jinan 250022, People's Republic of China

<sup>3</sup> Department of Spine, The Second Affiliated Hospital of Shandong University of Traditional Chinese Medicine, Jingba Road, Jinan, Shandong Province, People's Republic of China

## Background

Osteoporotic vertebral compression fracture (OVCF) is one of the most common fractures in patients with osteoporosis. Since Wilson et al. [1] first proposed the term of bone marrow edema (BME) in the imaging literature in 1988, magnetic resonance imaging (MRI) has been proven to be useful in detecting BME. Currently, BME on MRI has become the gold standard to diagnose acute/subacute OVCF [2]. It is defined as low signal intensity on T1-weighted imaging (T1WI) and high signal intensity on T2-weighted imaging (T2WI) and short time inversion recovery (STIR) [3].

As everyone knows, biopsy and pathological examination can reveal the microstructural changes of the fracture vertebrae. Particularly, the trabecular morphology, continuity, trabecular separation, necrotic tissue and new bone can be

observed in detail. It is of great significance to identify the pathogenesis, healing and prognosis of fracture [4].

However, there is a paucity of relevant literature discussing on the correlation of the quantitative BME pattern with the histopathologic findings of OVCF. Hence, the purpose of the study was to retrospectively investigate the relationship of BME signal intensities with histological characteristics in different fracture healing stages.

## Methods

### Patients

The study was approved by the Hospital Institutional Review Board, and informed consent was obtained from each patient. The patient-related data and imaging materials were obtained from the electronic medical record management system of Shandong provincial hospital affiliated to Shandong University.

Between June 2016 and October 2019 in our study, a total of 158 consecutive patients who underwent vertebroplasty for vertebral compression fracture were included in this retrospective study. Each bone biopsy specimen was derived from cancellous bone in the vertebral body and obtained during the procedure. All patients were symptomatic with the presence of persistent pain in the back and demonstrated BME in the fractured vertebral body on MRI. Since the statistical test hypothesis had independent observations, we selected only one vertebral fracture per patient in the analysis to reduce bias.

### Inclusion criteria

(1) Age over 50 years; (2) with back pain of less than 3 months' duration; (3) bone mineral density *T*-score  $\leq -2.5$ ; (4) single vertebral fracture; (5) a Numeric Rated Scale (NRS) pain score of 7 or more (out of 10); and (6) availability of complete clinical data.

### Exclusion criteria

(1) Inability to provide informed consent; (2) previous vertebroplasty on the affected vertebra; (3) progressive vertebral collapse, delayed union, neurological complications; (4) spine infections, vertebral tumors; (5) multiple vertebral fractures; and (6) treatment with glucocorticoids or anti-osteoporosis therapies.

### Staging

The fracture time was defined when the patient suddenly developed pain or obvious deterioration after minor or no

significant trauma. According to Diamond's staging criteria [5], all patients were divided into four stages: stage I (0 to 15 days), stage II (16 days to 30 days), stage III (31 days to 60 days) and stage IV (61 days to 90 days).

### BME evaluation

All patients underwent MRI to detect BME at the fractured vertebrae. MRI examinations were performed at 1.5 T (Signa; GE Medical Systems) according to the standard protocol at our institution. All sagittal T1WI, T2WI and STIR sequences were obtained with fast spin echo techniques. Two radiologists (with 8 and 6 years of experience in the interpretation of spinal images) retrospectively reviewed the spine MRI data independently, and any inconsistencies were resolved by consensus.

The sagittal images at the center of the vertebral bodies were selected and analyzed [6]. The location, shape and the intensity of BME on MRI were recorded. According to the proportion of volume of the fractured vertebral body on sagittal images, the pattern of BME was classified into three types: type 1, minor (1–24%); type 2, moderate (25–74%); and type 3, severe (75–100%), as described by Voormolen et al. [7].

### Bone biopsy

The bone biopsy was obtained through a pedicle approach. The positioning of the biopsy was standardized and localized at the fracture zone of the vertebral body.

The biopsy specimens consisting of a 0.5–1.0 cm core of cancellous bone were harvested, prepared with routine methods for decalcified paraffin histology, sectioned into 5- $\mu$ m-thick slices and stained with hematoxylin and eosin. The slices were observed under a microscope by an experienced pathologist.

### Quantitative histomorphometric analysis

According to the American Society for Bone and Mineral Research nomenclature [8], the histomorphometric parameters were expressed as follows: cancellous bone volume/tissue volume (BV/TV, %), woven bone volume/tissue volume (WBV/TV, %), endochondral bone volume/tissue volume (EBV/TV, %), granulation or fibrous tissue volume/tissue volume (FV/TV, %), osteoid volume/bone volume (OV/BV, %), osteoid surface/bone surface (OS/BS, %) and osteoid thickness ( $\mu$ m).

### Statistical analysis

The Statistical Package for the Social Sciences (SPSS) was used for statistical analysis (SPSS 20.0, SPSS Inc, Chicago

IL, USA). Quantitative results were compared by independent t test. Pearson's correlation coefficient was used to analyze the correlation with changes in BME percentage and other bone morphology parameters. Frequency analysis was performed with the Fisher's exact test or ANOVA.  $p < 0.05$  was considered to indicate a significant difference.

## Results

### Demographic data

Among the 158 patients, 6 patients treated with glucocorticoids were excluded from the study, and 6 patients were also excluded due to receiving established anti-osteoporosis therapies (e.g., fluoride, bisphosphonates, and anabolic steroids), 4 patients in whom a core bone biopsy failed to be obtained, 3 patients due to with pathologic fractures (malignancy), 9 patients due to multiple vertebral fractures, and 5 patients due to refusal.

A total of 125 patients qualified for the study, with 125 fractured vertebrae. The mean age was  $68.6 \pm 12.1$  years old, ranging from 54 to 90 years old. There were 90 females and 35 males. Seventy (56%) patients were classified as stage I, 29 (23.2%) as stage II, 12 (9.6%) as stage III and 14 (11.2%) as stage IV. The mean duration since fracture was  $10.2 \pm 5.8$  days for stage I,  $25.3 \pm 6.4$  days for stage II,  $48.8 \pm 11.7$  days for stage III and  $78.5 \pm 12.2$  days for stage IV. The difference was statistically significant ( $p = 0.007$ ). (Table 1).

**Table 1** Clinical demographics data in patients with OVCF classified according to different times since fracture

Demographics <sup>a</sup>	Fracture stage				
	Stage I	Stage II	Stage III	Stage IV	<i>p</i> value
Age (years)	$65.5 \pm 3$	$72.3 \pm 2$	$69.5 \pm 2$	$67.2 \pm 1$	0.2
sex ratio (men/women)	20:50	9:20	4:8	2:12	0.57
Lumbar spine bone density <i>T</i> -score	$-3.34 \pm 0.3$	$-2.67 \pm 0.2$	$-3.3 \pm 0.3$	$-3.61 \pm 0.3$	0.11
Mean time since fracture (days)	$10.2 \pm 0.8$	$25.3 \pm 0.4$	$48.8 \pm 0.7$	$78.5 \pm 0.2$	0.0007

<sup>a</sup>Values represent mean  $\pm$  1 S.E.M. OVCF: osteoporotic vertebral compression fractures

**Table 2** The vertebral BME pattern on T1WI images classified according to different times since fracture

BME pattern on T1WI MR images	Fracture staging				<i>p</i> value
	Stage I ( <i>n</i> = 70)	Stage II ( <i>n</i> = 29)	Stage III ( <i>n</i> = 12)	Stage IV ( <i>n</i> = 14)	
Type 1 minor (1–24%) ( <i>n</i> = 21)	6/70 (8.6%)	3/29 (10.3%)	5/12 (41.6%)	7/14 (50%)	0.002
Type 2 moderate (25–74%) ( <i>n</i> = 52)	27/70 (38.6%)	14/29 (48.2%)	5/12 (41.6%)	6/14 (42.8%)	0.531
Type 3 severe (75–100%) ( <i>n</i> = 52)	37/70 (52.8%)	12/29 (41.4%)	2/12 (16.7%)	1/14 (7.1%)	0.0015
Percentage of BME (%)	$75.35 \pm 21.9$	$69.72 \pm 22.54$	$40.91 \pm 28.85$	$28.64 \pm 15.91$	0.0008

Data in parentheses are fracture numbers. BME bone marrow edema

### BME evaluation

Various BME signals and forms were observed in the fractured vertebral bodies. The BME signal characteristics in the four stages were identified in the fractured vertebral body (Table 2).

**Stage I** Six (8.6%) fractured vertebrae showed a type 1 pattern, 27 (38.6%) showed a type 2 pattern, and 37 (52.8%) showed a type 3 pattern. The percentage of BME increased rapidly and reached the peak value ( $75.36 \pm 21.99\%$ ) in stage I. The signals on T1WI and T2WI were uniformly distributed, gradually transitioning to normal bone marrow, and demonstrated a morphological distribution of diffuse, uniform and unclear boundaries (Fig. 1a).

**Stage II** The percentage of BME decreased slightly ( $69.72 \pm 22.55\%$ ) at this stage after fracture. Three out of 29 (10.3%) fractured vertebrae showed a type 1 pattern, 14 (48.2%) showed a type 2 pattern, and 12 (41.4%) showed a type 3 pattern. The signals showed a heterogeneous distribution, including the inner points of the long T1 and T2 signals, and flaky short T1 or long T2 signals (Fig. 2a).

**Stage III** BME percentage ( $40.91 \pm 28.86\%$ ) continued to decrease compared to the percentage in the previous period. The range of edema was restricted and confined to the fracture zone. Five out of 12 (41.6%) fractured vertebrae showed a type 1 pattern, 5 (41.6%) showed a type 2 pattern, and 2 (16.7%) showed a type 3 pattern. Mixed signals: equal and low mixed signals in T1WI and mixed signals in low, equal and high forms in T2WI (Fig. 3a).

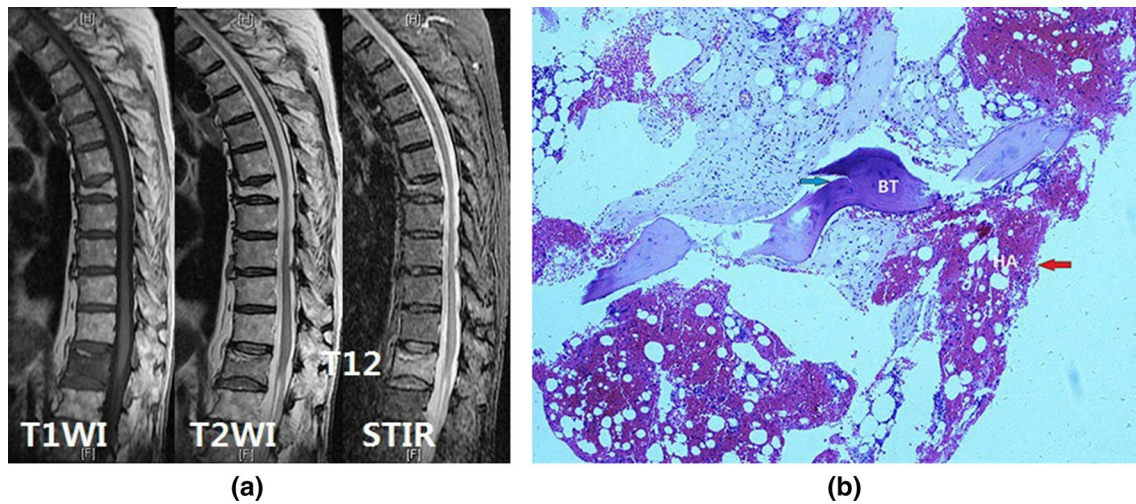


**Fig. 1 a** An 85-year-old man with OVCF at the T12 vertebral body. MRI shows a uniformly hypointense signal on T1WI, and a hyperintense signal on T2WI and STIR. A linear lucency shadow below the upper endplate represents the fracture line. Sagittal T1WI shows a type 3 BME pattern, and there is also an old, severe compression

fracture of T7. **b** Stage I is demonstrated by a fracture hematoma consisting of inflammatory cells during fracture healing, with trabecular breaks. OVCF: osteoporotic vertebral compression fracture, VCF: vertebral compression fracture, HA=hematoma, BT=normal bone trabecula

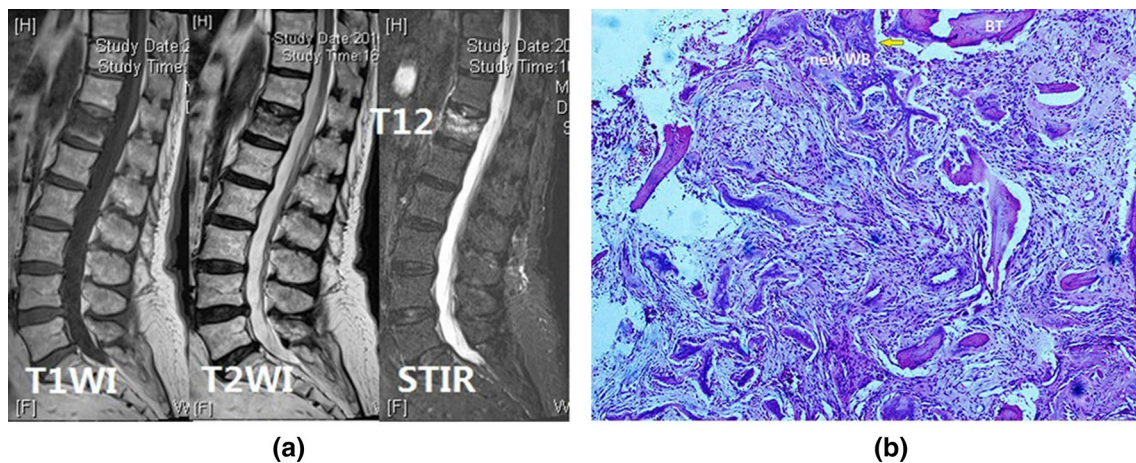


**Fig. 2 a** An 80-year-old woman with OVCF at the T12 vertebral body, depicting a heterogeneous distribution and a gradually decreased range of edema, with low signal changes in the fracture zone. **b** Stage II is demonstrated by organized hematoma, granula-

tion tissue and fibrous tissue proliferation, with chondrogenesis and osteoid matrix synthesis during fracture healing, and ‘new’ bone formation. OVCF: osteoporotic vertebral compression fracture, WB = woven bone, BT=normal bone trabecula

*Stage IV* The percentage of BME decreased to minimum value ( $28.65 \pm 15.91\%$ ) in stage IV. Seven out of 14 (50%) fractured vertebrae showed a type 1 pattern, 6 (42.8%) showed a type 2 pattern, and 1 (7.1%) showed a type 3 pattern. The incidence of the type 1 pattern increased from 8.5% to 50% ( $p=0.002$ ), and that of the type 3 pattern decreased from 52.8% to 7.1% ( $p=0.002$ ). A low signal area could be seen in the fracture zone on T1WI, with clear boundaries. The signals of T2WI and STIR were equivalent to those of adjacent normal vertebral bodies (Fig. 4a).

### Histopathological observation

The most predominant form of bone formation was cartilage formation within the marrow space. There was a significant difference between the histological changes in fracture healing. A significant overlap was observed between the various stages, with 87 patients (70%) having at least 2 or more stages in the same vertebral body (Table 3 and Fig. 5).

Using long bone fracture healing histological definitions [9], all biopsy specimens in the four stages were

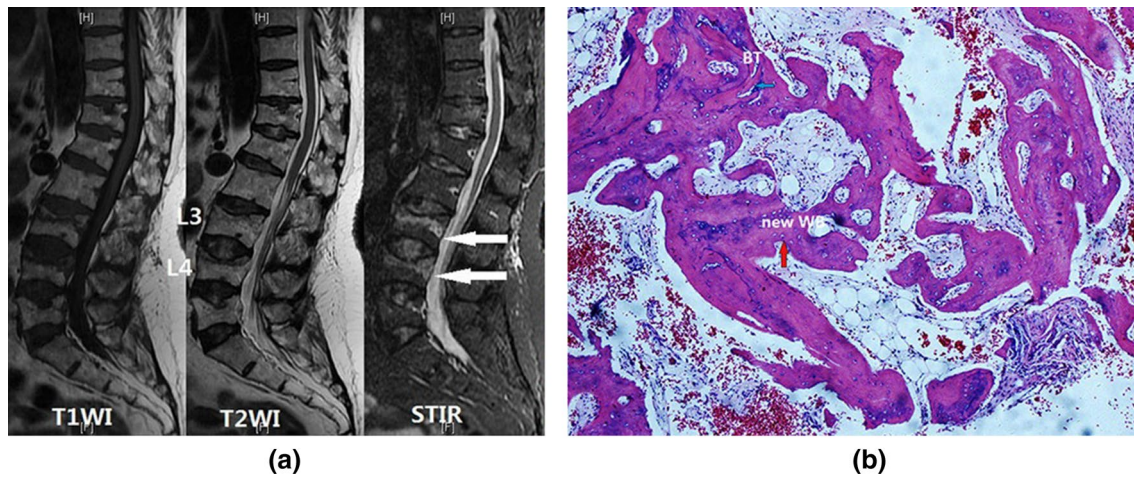


**Fig. 3 a** A 69-year-old woman with OVCF at the L3 and L4 vertebral bodies showing the type I BME pattern and biconcave deformity. The sagittal images show that the range of edema is narrowed down to the fracture line. **b** Stage III is demonstrated by new bone

formation in the marrow connecting the normal trabeculae. The net structure is initially formed. OVCF: osteoporotic vertebral compression fracture, WB = woven bone, BT = normal bone trabecula

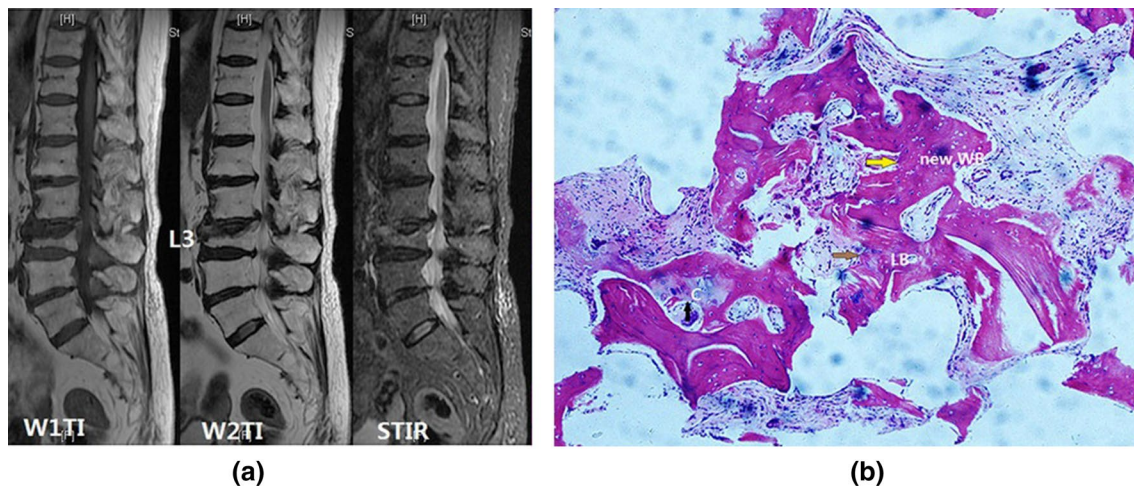


**Fig. 4 a** A 77-year-old woman with OVCF at the L3 vertebral body showing a hypointense signal on T1WI with a well-defined margin. The fracture body shows a hypointense signal on T1WI and an iso- or slightly hyperintense signal on T2WI and STIR. **b** Stage IV is demonstrated by bone modeling and remodeling during fracture healing.

Stress bone trabeculae appear, and woven bone is eventually replaced by lamellar bone; hematoma and fibrous small blood vessels are significantly reduced. OVCF: osteoporotic vertebral compression fracture, C = cartilage, WB = woven bone, LB = lamellar bone

characteristically described, which corresponded to the various BME signal characteristics in MR images.

**Stage I** The ratios of OV/BV and WBV/TV reached minimum values ( $1.9 \pm 0.4\%$  and  $0.13 \pm 0.05\%$ ) in stage I ( $p = 0.0006$  and  $0.000$ ). The trabecular cracks were more numerous, and the net structure was destroyed; there was a certain degree of fracture hematoma and fibrovascular stroma consisting of inflammatory cell infiltration during the fracture repair (Fig. 1b). This corresponded to the diffuse high signal intensity on T2WI in fractured vertebral bodies.

**Stage II:** A significantly greater FV/TV ( $50.2 \pm 7\%$ ) was found in stage II ( $p = 0.026$ ). The hematoma began to organize, the granulation tissue and fibrous tissue proliferated, more chondrocytes appeared between the fibrous tissues and proliferated to form focal cartilage, the bone matrix was synthesized and calcified, and calcium salt deposits formed primary bone trabeculae (Fig. 2b). The flaky short T1 or long T2 signals corresponded to granulation tissue or focal cartilage tissue, respectively.

**Table 3** Fracture callus morphometry in patients with vertebral fractures classified according to different times since fracture

Variable	Fracture stage				p value
	Stage I	Stage II	Stage III	Stage IV	
BV/TV (%)	12.5 ± 0.6	11.9 ± 0.5	13.7 ± 0.9	13.2 ± 1.2	0.204
OV/BV (%)	1.9 ± 0.4	4.5 ± 0.8	8.3 ± 1.2	6.8 ± 1.1	0.0006
WBV/TV (%)	0.13 ± 0.05	0.16 ± 0.2	5.6 ± 0.6	9.6 ± 1.0	0.000
FV/TV (%)	47.3 ± 5.4	50.2 ± 7	34.6 ± 3	21.9 ± 4.3	0.026
EBV/TV (%)	1.5 ± 0.5	7.4 ± 1.2	8.1 ± 0.9	2.7 ± 0.7	0.0002
OS/BS (%)	11.2 ± 0.5	20.5 ± 3.5	41.8 ± 2.7	39.2 ± 1.8	0.001

Cancellous bone volume/tissue volume (BV/TV, %), osteoid volume/bone volume (OV/BV, %), woven bone volume/tissue volume (WBV/TV, %), granulation or fibrous tissue volume/tissue volume (FV/TV, %), endochondral bone volume/tissue volume (EBV/TV, %), osteoid surface/bone surface (OS/BS, %), osteoid thickness (µm)

**Stage III** The ratio of OS/BS reached the peak value (41.8 ± 2.7%) in stage III ( $p = 0.001$ ). New bone formation in the marrow connected with old trabeculae, and the net structure was initially formed. Osteoblasts generated new bone and formed osteoid tissue, and then, calcium salt deposition occurred to form woven bone (Fig. 3b). The corresponding MRI findings showed that edema was confined to the fracture zone.

**Stage IV** The ratio of WBV/TV reached the peak value (9.6 ± 1.0%) in stage IV.

( $p = 0.001$ ). Bone modeling and remodeling were shown in the fracture callus, the bone matrix and bone trabeculae were significantly increased, and some trabeculae were mature and showed stress lines. There were a large number of bone marrow cells and vacuolar fat cells, and the degree of hematoma and the number of fibrous small blood vessels were significantly reduced (Fig. 4b). This pathological feature corresponded to the area where low signal intensity was observed on T1WI and T2WI.

### Relationship between BME and bone histomorphometry

The characteristics of BME during fracture healing and the histopathologic parameters were evaluated by a statistical model. Multivariate regression analysis showed that the fracture time was a constant significant predictor, and BME and histomorphometry showed obvious correlations in the fracture healing of acute OVCF. A significant and positive correlation was found between the BME percentage and the ratio of FV/TV ( $p < 0.0001$ ,  $r = 0.4882$ ). At the same time, BME had a significant negative correlation with the OV/BV ( $p < 0.0001$ ,  $r = -0.5389$ ), WBV/TV ( $p < 0.0001$ ,  $r = -0.5836$ ) and OS/BS ( $p < 0.0001$ ,  $r = -0.5727$ ) (Table 4 and Fig. 6).

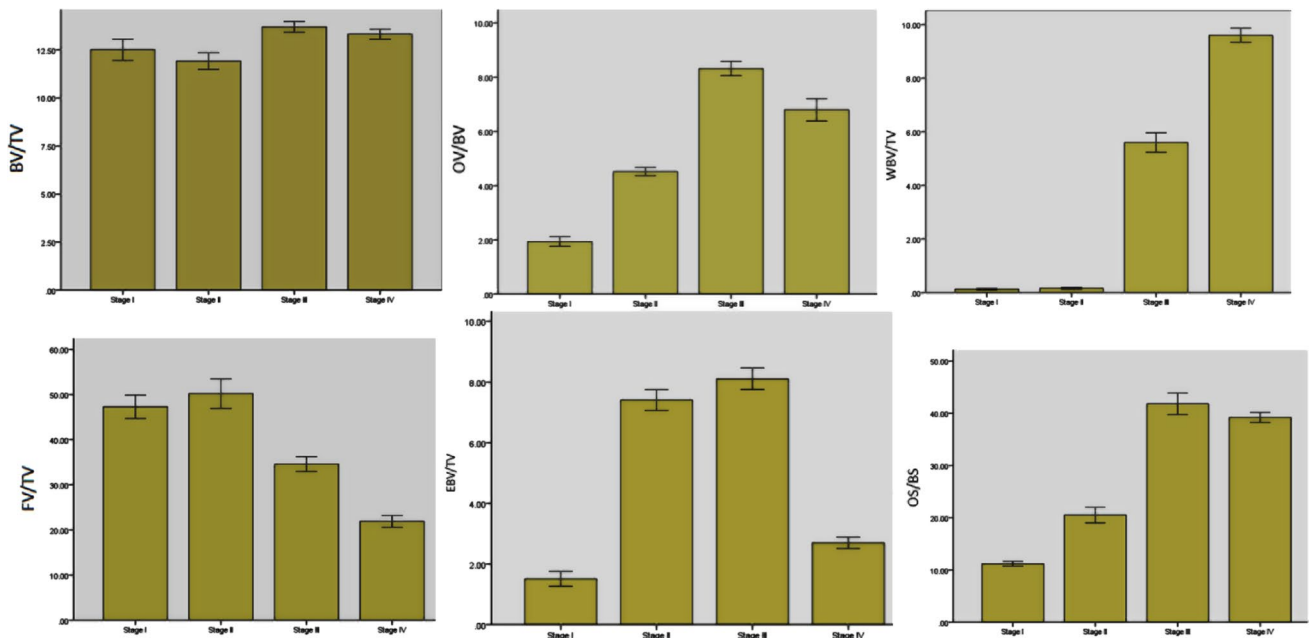


**Fig. 5** Fracture callus morphometry in patients during different time periods after osteoporotic vertebral compression fractures. The results of BV/TV, OV/BV, WBV/TV, FV/TV, EBV/TV and OS/BS are indicated as the mean ± standard error of mean (SEM)

**Table 4** Correlation analysis of BME and fracture callus morphometry according to different times since fracture

Variable	Clinical variable					
	BV/TV	OV/BV	WBV/TV	FV/TV	EBV/TV	OS/BS
<i>r</i> -value	−0.1745	−0.5389	−0.5836	0.4882	−0.2021	−0.5727
<i>p</i> -value	0.0517	0.0001	0.0001	0.0001	0.0238	0.0001

Cancellous bone volume/tissue volume (BV/TV, %), osteoid volume/bone volume (OV/BV, %), woven bone volume/tissue volume (WBV/TV, %), granulation or fibrous tissue volume/tissue volume (FV/TV, %), endochondral bone volume/tissue volume (EBV/TV, %), osteoid surface/bone surface (OS/BS, %), osteoid thickness ( $\mu\text{m}$ )

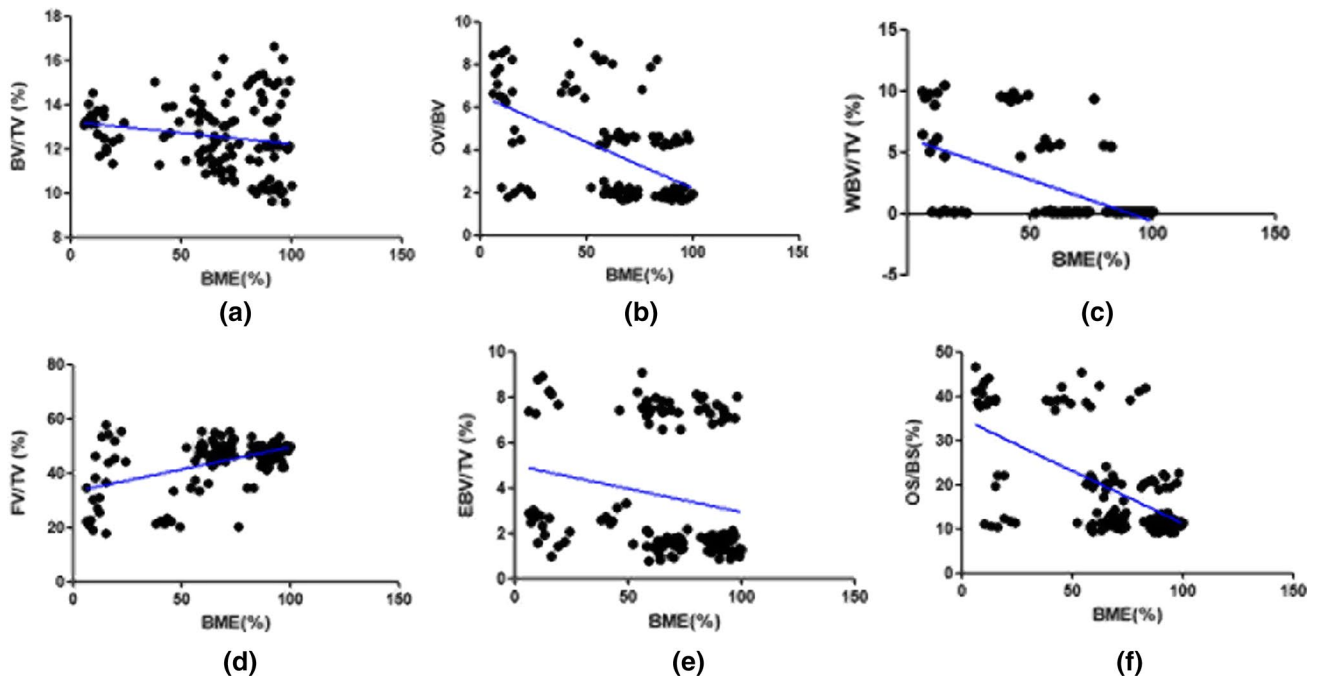


**Fig. 6** Scatter plots and linear regression values for all significant correlations with changes in BME. **a** There is no significant difference between BME and the BV/TV. **b** A significant negative correlation is shown between BME and the OV/BV. **c** A significant negative correlation is shown between BME and the WBV/TV. **d** A significant

positive correlation is shown between BME and the FV/TV. **e** A significant negative correlation is shown between BME and the EBV/TV. **f** A significant negative correlation is shown between BME and the OS/BS

## Discussion

Bone healing is difficult to assess on X-ray film or computer tomography (CT), especially for distinguishing the healing stage. MRI is very sensitive to the presence, location and extent of BME in fractured vertebrae [10]. BME can reveal the presence of pathological tissue conditions such as edema, hematoma and granulation, as well as the vascularity of the tissue [11]. The presence of BME in OVCF not only is considered one characteristic of acute/subacute fracture, but also is helpful for determining the stages of fracture healing through signal intensity changes [12].

Takahashi and Takahara [13, 14] made a simple classification of the time course of OVCF by MRI. Based on

mid-sagittal and bilateral parasagittal T1WI and T2WI sequences, the authors divided the signal changes within fractured vertebral bodies on MRI into three patterns: diffuse, confined and no signal change. The patterns of BME signal changes were mainly diffuse signal distributed in acute stage, with the progress of time, the signal area was restricted, and the distribution was mainly confined distributed. Consistent with the previous study, we also obtained similar observations.

To date, the healing process of long bone fractures has been well studied, but the histomorphometry of vertebral fractures during the healing process has been poorly reported [15]. Vernon-Roberts and Pirie [16] reported for the first time the healing of postmortem specimens of lumbar trabecular microfractures. Diamond et al. [5] made

histopathological observations of bone biopsies within 1–24 weeks after fracture. According to the analysis of different stages of fracture healing, the pathological changes inside the vertebral body are also different. However, Diamond neither studied the MRI signals at different fracture healing stages nor compared various MRI signal changes with the pathologic characteristics. To our knowledge, this report is the first study to investigate the correlation between BME and bone histomorphometry in (sub)acute osteoporotic vertebral compression fracture.

The healing mode of cancellous bone fractures is different from that of cortical bone [17]. The vertebral fracture healing process begins with an inflammatory response and local hematoma. Granulation tissue is gradually formed under hematoma organization, and thereafter, the cartilage matrix is produced by the action of fibroblasts. Cartilage is ossified by endochondral ossification, including the transformation of the fibrocartilaginous callus to mineralized cartilage and finally to bone [18]. The most fundamental steps are inflammation, repair and remodeling [19].

The histological features in stage I were characterized by hematoma and inflammatory exudative edema. With the increase in the water content of bone marrow, T1 and T2 relaxation times are prolonged, which present as low signals on T1WI, and high signals on T2WI and STIR sequence. The pathological changes in the acute phase appeared in a wide range around the fracture area and were not limited to the fracture line. The corresponding signals of BME presented a diffuse and uniform morphological distribution. Diffuse low signal changes might reflect bone bruising and trabecular cracks. On the contrary, hyperintense signal changes might be considered to be caused by hemorrhage after trabecular fracture [13]. This research shows that the signal in the edema period within 2 weeks after trauma appears to be the highest.

During 2 to 4 weeks after fracture, the traumatic edema has been gradually absorbed, water contents of tissue decreased, intensity of BME weakened, the proliferation of fibroblasts and new capillaries occurs, and the hematoma begins to become organized, with fibrin-rich granulation tissue and focal cartilage tissue [20]. Although a small amount of cartilage tissue was still found to be present in stage I ( $EBV/TV = 1.5 \pm 0.5\%$ ), the cartilage content increased rapidly ( $EBV/TV = 7.4 \pm 1.2\%$ ) in stage II. At the same time, the highest value was reached in stage III ( $EBV/TV = 8.1 \pm 0.9\%$ ). Granulation tissue contains a large number of neovascularization and fibrous connective tissue, showing slightly high signal on T2WI and STIR sequence, while cartilage is mainly composed of collagen, and its water content and corresponding signal intensity are lower than granulation tissue. It is manifested as a low or equal signal on T1WI and a slightly high signal on T2WI sequence. The difference in their scattered

distribution and maturity degree makes the signal uneven, which is manifested as a patchy, point or strip morphological distribution with gradually clear boundaries. The changes in the MRI signal in this stage mainly reflect early repair after fracture. In this stage, hematomas with more water content and areas of inflammatory reaction transit to cartilage with relatively less water content.

During 4 to 8 weeks after fracture, healing develops further, and a large amount of newly woven bone can be observed ( $WBV/TV = 5.6 \pm 0.6\%$ ). This means that endochondral bone is gradually mineralized, and calcium salt deposits gradually form the woven bone with less water content, which further reduces the signal intensity on MRI. However, the remnants of incomplete mineralized cartilage ( $EBV/TV = 8.1 \pm 0.9\%$ ) and non-thoroughly absorbed liquefied tissue cause abnormally high signals in fracture areas, so MRI signals show mixed signals. The appearance of such signals also indicates that cancellous bone fractures have not completely healed.

During 8 to 12 weeks after fracture, the trabecular bone increases and tends to mature, with partial adipose tissue changes, complete absorption of the edema and complete removal of the hematoma or tissue in the trauma area. A low-signal shadow with clear boundaries is visible on T1WI, which is thought to be due to traces of fracture during fracture healing process. Most of the high signals on T2WI and STIR disappear. The changes in MRI features described above are consistent with the histomorphological characteristics we observed. The content of fibrous tissue ( $FV/TV = 21.9 \pm 4.3\%$ ) and endochondral bone ( $EBV/TV = 2.7 \pm 0.7\%$ ), which are relatively rich in water, decreased significantly in this stage. In contrast, woven bone ( $WBV/TV = 9.6 \pm 1.0\%$ ) with less water content was significantly higher than in previous stages. There was also a non-significant increase in trabecular bone content ( $BV/TV = 13.2 \pm 1.2\%$ ). This further explains the disappearance of the high signal on T2WI and STIR from the histological point of view.

In recent years, although the majority of patients with OVCF who receive conservative treatment show successful pain relief [21, 22], minimally invasive spinal procedures such as vertebroplasty have been widely used in clinics and have been proven to be effective in treating OVCF [23].

*Stage I* indicates that fractured vertebrae are in the phase of acute edema with inflammatory edema stage. BME signals were mostly presents a diffuse distribution, and patients with severe pain. Conservative treatment (including pain relief and rehabilitation; assessment and management of the underlying osteoporosis) can be tried. If the patient is not suitable, minimally invasive surgical treatment (vertebroplasty) should be conducted as soon as possible.



**Stage II** With the gradual absorption of edema, the hematoma began to organize, granulation tissue and fibrous cartilage formed in large quantities. The signals showed a heterogeneous distribution, and the range is gradually restricted. Early weight bearing is not advisable. Conservative treatment may be continued, or vertebroplasty may be performed as soon as possible.

**Stage III** With the further development of fracture healing, the BME signal intensity was significantly weakened, and the range was restricted and confined to the fracture zone. Early weight bearing is also inappropriate at this time.

**Stage IV** suggests that most fractured vertebral bodies are basically healed, and the MRI signals tended to be consistent with those of the adjacent normal vertebral bodies; functional exercise can be gradually started at this time. However, if there are signs of vertebral collapse or abnormal signal changes in the fractured vertebral body, it usually indicates delayed healing of the fractured vertebra. Surgical treatment such as pedicle subtraction osteotomy (PSO) or vertebroplasty may be performed as soon as possible.

## Conclusions

The fracture time is considered to be an important predictor of the tissue healing stage in the vertebral body. MRI has a high diagnostic value for vertebral fracture and its healing degree, and its signal changes can reflect pathological changes to a certain extent, which is of great help in evaluating the healing status of vertebral fractures, and secondary pathological changes. If BME in OVCF can be predicted at an early stage, more active treatment can be initiated relatively early. Further studies comparing the various imaging findings of intravertebral cleft with its histological characteristics would allow for evaluating the pathological development of osteoporotic vertebral fracture by non-invasive methods.

**Acknowledgements** We would like to thank Xiaoyang Liu for his help in professional linguistic correction.

**Author contributions** YZ, HQ, JS and JW contributed to conceptualization. JX and HQ were involved in data curation. JX, YZ and HQ contributed to formal analysis, investigation and methodology. YZ and HQ were involved in software. JS contributed to supervision. JS and JW were involved in validation. YZ, HQ and JS contributed to visualization. YZ, HQ, JX and JS were involved in writing—original draft. YZ, JX and JS contributed to writing—review and editing.

**Funding** This article did not receive any funding and grants from agencies.

## Declarations

**Conflict of interest** We declare that this article has not been published before in any language, is not being considered for publication elsewhere and has been read and approved by all authors. Each author contributed significantly to one or more aspects of the study. The authors received no specific funding for this work. There are no conflicts of interest around this study. The authors have full control of all primary data and agree to allow the journal to review their data if requested.

**Ethical approval** The study was approved by the Hospital Institutional Review Board, and informed consent was obtained from all patients. The informed consent provided by participants was written, and they consented to the use of their medical information for research purposes. Prior to access, all patient data were completely anonymous.

## References

1. Wilson AJ (1988) Transient osteoporosis. transient bone marrow edema? *Radiology* 167:757–760. <https://doi.org/10.1148/radiology.167.3.3363136> (PMID: 3363136)
2. Jung HS, Jee WH, McCauley TR, Ha KY, Choi KH (2003) Discrimination of metastatic from acute osteoporotic compression spinal fractures with MR imaging. *Radiographics* 23(1):179–187. <https://doi.org/10.1148/rg.231025043> (PMID: 12533652)
3. Piazzolla A, Solarino G, Lamartina C, Giorgi SD, Bizzoca D, Berjano P (2015) Vertebral bone marrow edema (VBME) in conservatively treated acute vertebral compression fractures (VCFs): evolution and clinical correlations. *Spine (Phila Pa 1976)* 40:E842–E848. <https://doi.org/10.1097/brs.0000000000000973> (PMID:25946722)
4. Aspenberg P, Sandberg O (2013) Distal radial fractures heal by direct woven bone formation. *Acta Orthop* 84(3):297–300. <https://doi.org/10.3109/17453674.2013.792769> (PMID: 23570338)
5. Diamond TH, Clark WA, Kumar SV (2007) Histomorphometric analysis of fracture healing cascade in acute osteoporotic vertebral body fractures. *Bone* 40:775–780. <https://doi.org/10.1016/j.bone.2006.10.009> (PMID: 17141596)
6. Kazawa N (2012) T2WI MRI and MRI-MDCT correlations of the osteoporotic vertebral compressive fractures. *Eur J Radiol* 81:1630–1636. <https://doi.org/10.1016/j.ejrad.2011.04.052> (PMID: 21636232)
7. Voormolen MHJ, Rooij WJV, Graaf YVD, Lohle PNM, Sluzewski M (2006) Bone marrow edema in osteoporotic vertebral compression fractures after percutaneous vertebroplasty and relation with clinical outcome. *Ajnr Am J Neuroradiol* 27:983–988. <https://doi.org/10.1016/j.neuroimage.2005.11.053> (PMID: 16687528)
8. Gerstenfeld LC, Wronski TJ, Hollinger JO, Einhorn TA (2005) Application of histomorphometric methods to the study of bone repair. *J Bone Miner Res* 20:1715–1722. <https://doi.org/10.1359/JBMR.050702> (PMID: 16160729)
9. Einhorn TA (1998) The cell and molecular biology of fracture healing. *Clin Orthop Relat R* 355S(355):S7–21. <https://doi.org/10.1097/00003086-199810001-00003> (PMID: 9917622)
10. Lee JM, Lee YS, Kim YB, Park SW, Kang DH, Lee SH (2017) What effects does necrotic area of contrast-enhanced MRI in osteoporotic vertebral fracture have on further compression and clinical outcome? *J Korean Neurosurg* 60:181–188. <https://doi.org/10.3340/jkns.2016.0707.015> (PMID: 28264238)
11. Taljanovic MS, Graham AR, Benjamin JB, Gmitro AF, Krupinski EA, Schwartz SA, Hunter TB, Resnick DL (2008) Bone marrow edema pattern in advanced hip osteoarthritis: quantitative assessment with magnetic resonance imaging and correlation with

- clinical examination, radiographic findings, and histopathology. *Skeletal Radiol* 37(5):423–431. <https://doi.org/10.1007/s00256-008-0446-3> (PMID: 18274742)
12. Phillips FM, Ho E, Campbell-Hupp M, McNally T, Todd Wetzel F, Gupta P (2003) Early radiographic and clinical results of balloon kyphoplasty for the treatment of osteoporotic vertebral compression fractures. *Spine (Phila Pa 1976)* 28:2260–2265. <https://doi.org/10.1097/01.brs.0000085092.84097.7b> (PMID: 14520041)
  13. Takahashi S, Hoshino M, Takayama K, Iseki K, Sasaoka R, Tsujio T, Yasuda H, Sasaki T, Kanematsu F, Kono H, Toyoda H, Nakamura H (2017) Time course of osteoporotic vertebral fractures by magnetic resonance imaging using a simple classification: a multicenter prospective cohort study. *Osteoporos Int* 28(2):473–482. <https://doi.org/10.1007/s00198-016-3737-x> (PMID: 27577726)
  14. Takahara K, Kamimura M, Nakagawa H, Hashidate H, Uchiyama S (2007) Radiographic evaluation of vertebral fractures in osteoporotic patients. *J Clin Neurosci* 14(2):122–126. <https://doi.org/10.1016/j.jocn.2005.11.050> (PMID: 17161286)
  15. Mukherjee S, Thakur B, Bhagawati D, Bhagawati D, Akmal S, Arzoglou V (2014) Utility of routine biopsy at vertebroplasty in the management of vertebral compression fractures: a tertiary center experience. *J Neurosurg Spine* 21(5):687–697. <https://doi.org/10.3171/2014.7.spine121015> (PMID: 25127432)
  16. Vernon-Roberts B, Pirie CJ (1973) Healing trabecular microfractures in the bodies of lumbar vertebrae. *Ann Rheum Dis* 32:406–412. <https://doi.org/10.1136/ard.32.5.406> (PMID: 4270883)
  17. Bogoch E, Gschwend N, Rahn B, Moran E, Perren S (1993) Healing of cancellous bone osteotomy in rabbits—part II: local reversal of arthritis-induced osteopenia after osteotomy. *J Orthop Res* 11(2):292–298. <https://doi.org/10.1002/jor.1100110217> (PMID: 8483042)
  18. Braun W, Ruter A (1996) Fracture healing. morphologic and physiologic aspects. *Unfallchirurg* 99:59–67 (PMID: 8850081)
  19. Remedios A (1999) Bone and bone healing. *Vet Clin N Am-Small* 29:1029–1044. [https://doi.org/10.1016/S0195-5616\(99\)50101-0](https://doi.org/10.1016/S0195-5616(99)50101-0) (PMID: 10503283)
  20. Greenbaum MA, Kanat IO (1993) Current concepts in bone healing. *J Am Podiat Med Assn* 83:123–129 (PMID: 11344980)
  21. Yang H, Liang C, Zheng Z, Yin G, Zou J (2017) Therapeutic effects analysis of percutaneous kyphoplasty for osteoporotic vertebral compression fractures: a multicentre study. *J Orthop Transl* 11:73–77. <https://doi.org/10.1016/j.jot.2017.04.003> (PMID: 29662771)
  22. Venmans A, Klazen CA, Lohle PN, Mali WP, van Rooij WJ (2012) Natural history of pain in patients with conservatively treated osteoporotic vertebral compression fractures: results from VERTOS II. *AJNR Am J Neuroradiol* 33:519–521. <https://doi.org/10.3174/ajnr.a2817> (PMID: 22116114)
  23. Jing Z, Sun Q, Dong J, Meng F, Nan F (2017) Is it beneficial to reuse the balloon in percutaneous kyphoplasty for the treatment of non-neoplastic vertebral compression fractures? *Med Sci Monit* 23:5907–5915. <https://doi.org/10.12659/MSM.905161> (PMID: 29236682)

**Publisher's Note** Springer Nature remains neutral with regard to jurisdictional claims in published maps and institutional affiliations.